SPANDIDOS PUBLICATIONS

MOLECULAR MEDICINE REPORTS 17: 1933-1939, 2018

Effect of moesin phosphorylation on high-dose sphingosine-1-phosphate-induced endothelial responses

YAN XIAO[1*], JIE WU[1,2*], YONGJUN YUAN[1], XIAOHUA GUO[1], BO CHEN[1] and QIAOBING HUANG[1]

[1]Department of Pathophysiology, Key Laboratory for Shock and Microcirculation Research of Guangdong; [2]First Clinical College of Medicine, Southern Medical University, Guangzhou, Guangdong 510515, P.R. China

Received March 24, 2017; Accepted August 18, 2017

DOI: 10.3892/mmr.2017.8029

Abstract. It was previously reported that low-dose sphingosine-1-phosphate (S1P) enhanced endothelial barrier integrity, whereas high-dose S1P induced endothelial monolayer hyperpermeability responses. A number of studies have revealed the underlying molecular mechanisms of the physiological-dose of S1P on barrier-protective effect. However, little work has been performed to determine the effect of S1P-induced endothelial barrier responses. In the present study, the role of moesin phosphorylation in excessive S1P-induced endothelial hyperpermeability was investigated by western blotting, fluorescence staining and transendothelial electrical resistance detection. It was revealed that S1P induced moesin phosphorylation in a time- and concentration-dependent manner. In addition, it was confirmed that high-dose S1P-induced moesin phosphorylation occurred via S1P receptor 2 (S1PR2). Moesin phosphorylation was required for S1P-induced F-actin rearrangement and endothelial barrier disruption. The results suggested that the S1PR2-moesin axis is involved in high-dose S1P-induced endothelial barrier responses. The results of the present study may provide novel therapeutic targets for endothelial injury-associated vascular disorders.

Introduction

The vascular endothelium forms a semi-permeable barrier between blood and tissue compartments, and serves an important role in regulating vascular physiological functions. However, the disruption of the endothelial barrier, marked by an increased vascular permeability, contributes to the pathogenesis of various inflammatory disease processes (1).

Sphingosine-1-phosphate (S1P), a bioactive sphingolipid abundant in plasma, is emerging as a potent modulator of a variety of biological functions in endothelial cells, including cell cytoskeleton regulation, cellular locomotion, angiogenesis and vascular maturation (2). Thrombocyte was originally considered as the primary source of S1P (3). However, previous work has suggested that the main source of plasma S1P is erythrocytes, which mediates the release of S1P independent of stimuli and may serve as a 'buffer system' against S1P depletion (4). The next candidate for non-hematopoietic derived S1P is endothelial cells, which contribute to 40% of plasma S1P in mice (5,6).

It was previously demonstrated that S1P may be protective in burn injury by enhancing the endothelial barrier function (7). Mounting evidence has demonstrated that S1P mediates different cellular responses by interacting with S1P receptors (S1PRs). The primary receptors expressed in endothelial cells are S1PR1, S1PR2 and S1PR3 (8). Among these, S1PR1 activates the Rac signaling pathway, which promotes vascular integrity (9). By contrast, S1PR2 activates the Rho pathway and leads to disruption of endothelial barrier integrity. Previous studies have revealed that S1PR2 is an attractive target for the treatment of disorders of both macro- and micro-vasculature (2,10,11). Kim *et al* (12) demonstrated that S1PR2 serves a critical role in the disruption of cerebrovascular integrity in experimental stroke models. Evidence has demonstrated that S1PR2 serves a key role in the permeability and inflammatory responses of the vascular endothelium during endotoxemia (13). It was previously reported that low-dose S1P enhanced endothelial barrier integrity through S1PR1, whereas high-dose S1P induced endothelial hyperpermeability via S1PR2 (14). Consistently, Sammani *et al* (15) revealed the therapeutic effects of S1PR1 in ameliorating inflammatory lung injury, whereas by contrast, the activation of S1PR2 or S1PR3 induced significant alveolar and vascular barrier disruption.

Ezrin, radixin and moesin (ERM) proteins organize the cortical cytoskeleton by linking filamentous actin to the plasma membrane. S1P promotes ERM translocation to the cell periphery and its subsequent phosphorylation on a threonine residue (16). These actin-binding proteins are engaged differently in endothelial barrier responses. A previous

Correspondence to: Professor Qiaobing Huang, Department of Pathophysiology, Key Laboratory for Shock and Microcirculation Research of Guangdong, Southern Medical University, Tonghe, 1023 Shatai Road, Guangzhou, Guangdong 510515, P.R. China
E-mail: bing@smu.edu.cn

*Contributed equally

Key words: sphingosine-1-phosphate, Sphingosine-1-phosphate receptor 2, moesin, endothelial responses

study demonstrated that moesin promoted thrombin-induced endothelial barrier dysfunction, whereas radixin exerted the opposite effect (17).

Moesin is the primary ERM protein expressed in endothelial cells. It was previously demonstrated that moesin phosphorylation was required in advanced glycation end products (AGEs)-induced F-actin rearrangement and hyperpermeability responses in endothelial cells (18). In the present study, it was questioned whether moesin phosphorylation was also involved in excessive S1P-induced endothelial barrier disruption. Therefore, the role of moesin phosphorylation in modulating high-dose S1P-induced endothelial hyperpermeability responses was investigated. The present study may contribute to the identification of novel drug targets for the treatment of vascular disorders.

Materials and methods

Reagents. Human umbilical vein endothelial cells (HUVECs) were purchased from Scien Cell Research Laboratories (Carlsbad, CA, USA). Dulbecco's modified Eagle's medium (DMEM)/F12 medium, fetal bovine serum (FBS), trypsin, glutamine, penicillin and streptomycin were all from Gibco; Thermo Fisher Scientific, Inc. (Waltham, MA, USA). S1P was obtained from Sigma-Aldrich; Merck KGaA (Darmstadt, Germany). The S1PR1 antagonist W146 was from Avanti Polar Lipids, Inc. (Alabaster, AL, USA). The S1PR2 antagonist, JTE013, and the S1PR3 antagonist, CAY10444, were purchased from Cayman Chemical Company (Ann Arbor, MI, USA). An antibody against phosphorylated (p)-moesin (Thr558) was from Santa Cruz Biotechnology, Inc. (Dallas, TX, USA; cat. no. sc-12895); a moesin antibody was from Cell Signaling Technology, Inc. (Danvers, MA, USA; cat. no. 3150). An anti-β-actin antibody was from OriGene Technologies, Inc. (Beijing, China; cat. no. TA310155). The secondary antibodies, rabbit anti-mouse IgG horseradish peroxidase-conjugated (HRP) antibody (cat. no. bs-0296R-HRP) and goat anti-rabbit IgG HRP-conjugated antibody (cat. no. bs-0295G-HRP) were from Beijing Biosynthesis Biotechnology Co., Ltd. (Beijing, China). Human moesin small interfering (si)RNA and control nonsense siRNA were purchased from Shanghai GenePharma Co., Ltd. (Shanghai, China). Rhodamine-phalloidin recognizing F-actin was obtained from Molecular Probe; Thermo Fisher Scientific, Inc. (cat. no. R415). Biochemical reagents were obtained from Sigma-Aldrich unless otherwise indicated.

Cell culture. HUVECs were cultured in DMEM/F12 containing 10% FBS at 37˚C in a humidified atmosphere with 5% CO_2 and 95% air. In all experiments, HUVECs were grown to 90% confluence and starved of serum for 12 h. HUVECs were then stimulated with 10 μmol/l S1P for 0, 5, 10, 20, 40, 60 and 90 min, respectively. In order to study the effect dose effect, HUVECs were also stimulated with 0, 0.5, 1, 5 and 10 μmol/l S1P for 20 min. The following investigations were performed under S1P (10 μmol/l) treatment at 37˚C for 20 min; HUVECs treated with DMEM onlly were used as control. For detection of the effects on S1P receptors in HUVEC responses, specific antagonists of S1PR1 (10 μmol/l), S1PR2 (10 μmol/l) and S1PR3 (10 μmol/l) were each added to HUVECs at 37˚C for 30 min before the relevant S1P application.

Transfection of siRNA. HUVECs were seeded into 6-well plates at 70-80% confluence. After 24 h, HUVECs were incubated at 37˚C with siRNA Mate Transfection reagent (Shanghai Gene Pharma Co., Ltd.) and siRNA targeting moesin (sense 5'-GGGAUGUCAACU GACCUAAdTdT-3' and antisense 5'-UUAGGUCAGUUG ACAUCCCdTdG-3'), or control nonsense siRNA (sense 5'-UUCUCCGAACGUGUCACGUUTdTdG-3' and antisense 5'-ACGUGACACGUUCGGAGAATTdTdG-3'), according to the manufacturer's protocol. The transfected cells were harvested 48-72 h later.

Western blotting. Total cellular extracts were prepared using lysis buffer (20 mmol/l Tris at pH 7.4, 2.5 mmol/l EDTA, 1% Triton X-100, 1% deoxycholic acid, 0.1% SDS, 100 mmol/l NaCl, 10 mmol/l NaF and 1 mmol/l Na_3VO_4) supplemented with protease and phosphatase inhibitors. Total proteins concentrations were measured by Bicinchoninic Acid assay, and then 30 μg of protein samples were subjected to 12% SDS-PAGE separation, and transferred onto polyvinylidene difluoride membranes. After blocking with 5% bovine serum albumin (BSA; GBCBIO Technologies, Inc., Guangdong, China), the membranes were incubated with primary antibodies against p-moesin, moesin and β-actin at 1:1,000 dilution at 4˚C overnight, with agitation. Following washing three times with TBST containing 0.1% Tween-20 (each time for 10 min), membranes were probed with an HRP-conjugated rabbit anti-mouse or goat anti-rabbit IgG antibody according to the source of the primary antibody at 1:8,000 dilution at room temperature for 1 h. After washing the membrane three times with TBST for 10 min each time, the protein bands were visualized using a chemiluminescence reagent (EMD Millipore, Billerica, MA, USA). Images were acquired using a Kodak IS4000R Imaging instrument (Kodak, Rochester, NY, USA), and then densitometric analysis was performed using ImageJ version 1.48i (National Institutes of Health, Bethesda, MD, USA).

Fluorescence staining. The distribution of the cytoskeletal F-actin in HUVECs was determined. HUVECs were plated on gelatin-coated glass-bottom microwell plates (MatTek Corporation, MA, USA) and cultured until 70-80% confluent. Cells were transfected with moesin siRNA or control nonsense siRNA, which was followed by further treatment with or without S1P. The untransfected cells treated with DMEM alone were used as control. Then, the medium was removed, and the cells were washed with PBS and permeabilized for 15 min at room temperature in PBS containing 3.7% formaldehyde and 0.5% Triton X-100. Subsequently, cells were washed with PBS twice and blocked in 5% BSA at room temperature for 1 h. After a thorough wash in PBS, the cells were stained with a conjugated rhodamine-phalloidin antibody (2 U ml^{-1}) at room temperature for 1 h. Cells were further incubated with diamidino-2-phenylindole (DAPI; 1:1,000) at room temperature for 15 min and then washed with PBS again. DAPI was used to stain nuclear DNA. The staining results were imaged using a Zeiss LSM780 laser confocal scanning microscope (Zeiss GmbH, Jena, Germany), and analyzed using ImageJ version 1.48i (National Institutes of Health).

Transendothelial electrical resistance (TER). TER of the HUVEC monolayer was determined using a STX2 electrode and EVOM^2 meter according to the manufacturer's protocol (World Precision Instruments, Sarasota, FL, USA) (19). Briefly, HUVECs were seeded at 0.5x10^5/well in gelatin-coated, 6.5 mm Transwell filters (0.4-mm pore size) until confluent. Resistance values of multiple Transwell inserts within an experimental group were measured sequentially and the mean was expressed in the common unit (Ωcm^2) after subtraction of the value of a blank cell-free filter.

Statistical analysis. All data are expressed as the mean ± standard deviation from at least three independent experiments and analyzed using SPSS version 16.0 software (SPSS, Inc., Chicago, IL, USA). Statistical comparisons were performed using a one-way analysis of variance with Bonferroni post hoc test. $P<0.05$ was considered to indicate a statistically significant difference.

Results

S1P induces moesin phosphorylation in HUVECs. Previously published results suggested that moesin is phosphorylated in AGE-induced endothelial barrier dysfunction (18,20). To determine whether moesin phosphorylation serves a role in S1P-mediated endothelial hyperpermeability, moesin phosphorylation levels were measured after S1P treatment. HUVECs were incubated with a high dose of S1P (10 μmol/l) for different durations, and then p-moesin expression levels were determined by western blotting. The results demonstrated that phosphorylation of moesin was significantly enhanced after a 5-min S1P treatment compared with untreated cells, and gradually reached a peak at 20 min, before the expression decreased to a relatively stable level until 90 min S1P stimulation (Fig. 1A). The influence of S1P treatment at different doses on moesin phosphorylation were also investigated in endothelial cells after S1P incubation for 20 min. It was demonstrated that the phosphorylation levels of moesin were significantly increased by S1P in a concentration-dependent manner compared with untreated cells, ranging from 0.5 to 10 μmol/l (Fig. 1B). These results suggested that S1P induces moesin phosphorylation in a time- and dose-dependent manner.

High-dose S1P mediates moesin phosphorylation via S1PR2. It was previously demonstrated that low-dose S1P (0.5-1 μmol/l) enhances endothelial barrier integrity via S1PR1, whereas high-dose S1P (5-10 μmol/l) induced endothelial monolayer hyperpermeability responses via S1PR2 (14). Given that moesin phosphorylation is involved in endothelial barrier disruption, it was questioned whether S1PR2 is required for S1P-induced moesin phosphorylation. Thus, HUVECs were subjected to S1P treatment (10 μmol/l) for 20 min. In order to confirm the effects of different S1PRs, specific S1PR antagonists were used. Pretreatment of the S1PR2 antagonist (JTE013) significantly attenuated moesin phosphorylation compared with the S1P group. However, the S1PR1 antagonist (W146) and S1PR3 antagonist (CAY10444) did not affect high-dose S1P-induced moesin phosphorylation (Fig. 2). This suggested that S1PR2 is required to enhance moesin phosphorylation induced by high-doses of S1P.

Moesin phosphorylation is involved in high-dose S1P-induced endothelial barrier dysfunction. To determine whether moesin phosphorylation is involved in high-dose S1P-induced responses in endothelial cells, siRNA targeting moesin was used. HUVECs transfected with moesin siRNA exhibited significantly reduced moesin expression levels compared with untransfected control cells, whereas negative control siRNA had no effect on moesin expression (Fig. 3A). Consistent with the above findings, high-dose S1P increased moesin phosphorylation, however, knockdown of moesin reduced the levels of phosphorylated moesin in HUVECs treated with high-dose S1P (Fig. 3B).

Next, it was determined whether moesin phosphorylation was involved in the structural and functional changes in high-dose S1P-treated endothelial cells. The role of moesin in modulating endothelial cell structural responses induced by S1P was examined by visualizing the distribution of F-actin (Fig. 4A). When compared with the control, the application of high-dose S1P resulted in the disorganization of F-actin and the formation of stress fibers, as well as the opening of intercellular gaps (panel 2 in Fig. 4A). This effect was markedly attenuated by moesin siRNA (panel 4 in Fig. 4A), while the application of 10 μmol/l S1P in control siRNA-treated cells caused the same polymerization of F-actin and formation of stress fibers (panel 6 in Fig. 4A) as S1P-treated alone. No significant alterations were observed in the moesin siRNA or the control siRNA groups. These results suggested that moesin may have a critical role in mediating F-actin rearrangement induced by high-dose S1P.

To further confirm the effect of moesin on S1P-induced endothelial barrier responses, a TER test was performed (Fig. 4B). The monolayer TER was measured intermittently within 90 min. Accordingly, compared with control group, the S1P-treated and S1P+NC siRNA groups exhibited a significant decrease in the TER value and reached a plateau at 20 min, and then restored to a level lower than 0 min in the later stage. Pretreatment with moesin siRNA attenuated the S1P-induced decline in TER and the value at 90 min was similar to the value to 0 min. No significant differences were observed between the TER value in the moesin siRNA group or the NC siRNA group. Taken together, it was concluded that moesin phosphorylation serves an important role in S1P-induced F-actin rearrangement and endothelial barrier disruption.

Discussion

Physiological plasma levels of circulating S1P are vasculoprotective, whereas abnormal activation of S1P signaling is associated with a diverse range of diseases, including diabetes, fibrosis and cancer (21,22). In certain pathological conditions, the serum S1P concentration may be increased and contribute to vascular hyperpermeability responses. It was previously demonstrated that physiological concentrations of S1P, ranging from 0.1 to 1 μmol/l, contribute to endothelial barrier-protective responses via S1PR1. By contrast, high concentrations of S1P (>5 μmol/l) hampers endothelial barrier integrity via S1PR2 (14). The underlying molecular mechanisms of the protective role of physiological-dose S1P in endothelial integrity enhancement have been widely reported (23-26). However,

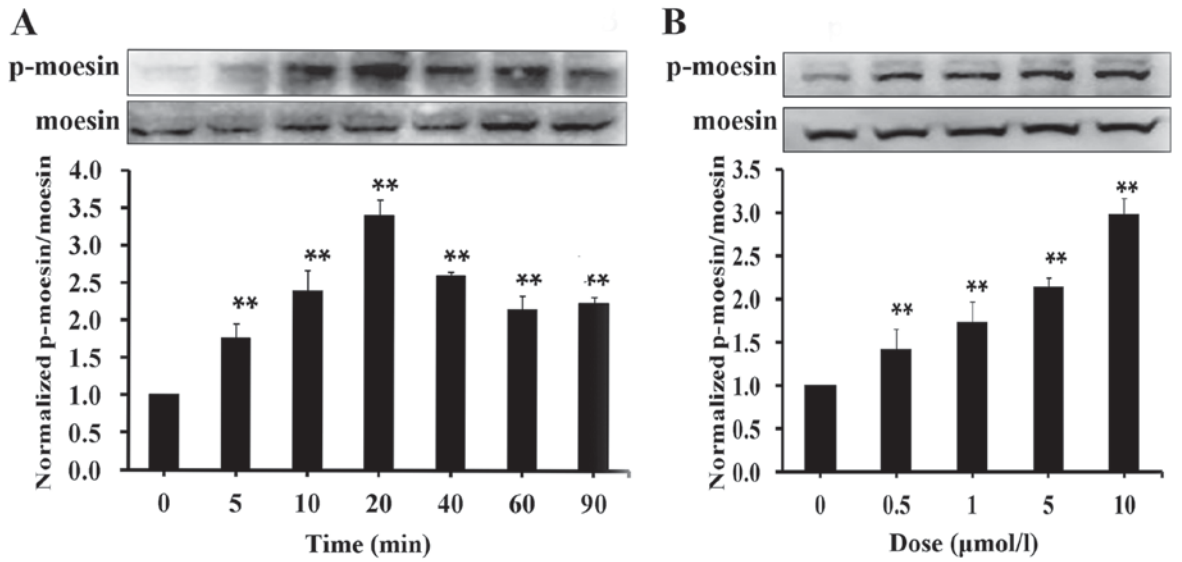

Figure 1. S1P induces moesin phosphorylation in a time- and concentration-dependent manner. HUVECs were treated with (A) 10 μmol/l S1P for the indicated times or (B) stimulated with S1P at the indicated doses for 20 min. The expression levels of threonine-phosphorylated moesin or total moesin were examined using western blot analysis. The results are expressed in mean ± standard deviation from three independent experiments. **P<0.01 vs. untreated control. p-phosphorylated; S1P, sphingosine-1-phosphate.

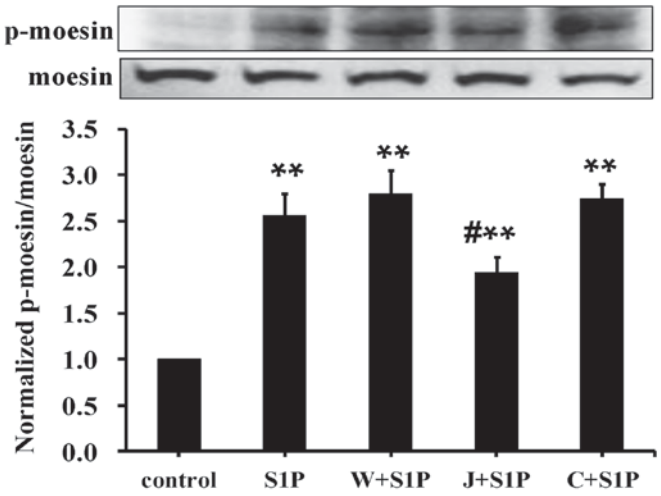

Figure 2. Involvement of S1PR2 in high-dose S1P-induced moesin phosphorylation. HUVECs were pretreated with either each of the S1PR1, S1PR2 or S1PR3 antagonists for 30 min, or without antagonist treatment, prior to the addition of 10 μmol/l S1P for 20 min. p-moesin or total moesin was examined using western blot analysis. The results are expressed as the mean ± standard deviation from three independent experiments. **P<0.01 vs. untreated control; $^{\#}$P<0.05 vs. S1P. p-, phosphorylated; S1P, sphingosine-1-phosphate; W+S1P, S1PR1 antagonist W146 and sphingosine-1-phosphate; J+S1P, S1PR2 antagonist JTE013 and sphingosine-1-phosphate; C+S1P, S1PR3 antagonist CAY10444 and sphingosine-1-phosphate; S1PR1, sphingosine-1-phosphate receptor 1; S1PR2, sphingosine-1-phosphate receptor 2; S1PR3, sphingosine-1-phosphate receptor 3.

signaling pathways underlying high-dose S1P-induced endothelial barrier dysfunction remains to be fully clarified.

Moesin is the primary ERM protein expressed in endothelium. Phosphorylation of moesin is critically implicated in endothelial barrier dysfunction. Previously, the role of moesin phosphorylation in AGE-induced endothelial hyperpermeability was described (18). The present study investigated the effect of moesin phosphorylation on excessive S1P-induced endothelial barrier responses. S1P induced significant moesin phosphorylation in a time- and dose-dependent manner. High-dose S1P induced sustained threonine phosphorylation of moesin, which reached maximum levels at 20 min and remained elevated for ≥90 min. These results were consistent with the prior observation that physiological doses of S1P induced a significant elevation in moesin phosphorylation (27). However, an S1PR1 specific agonist, SEW2871, had no effect on moesin phosphorylation (27). In addition, siRNA depletion of S1PR1 failed to attenuate S1P-induced ERM phosphorylation, whereas antagonists for S1PR2 (JTE013) or S1PR3 (CAY10444) exhibited dramatic decrease of ERM phosphorylation (27). These results suggested that S1PR2 and/or S1PR3, but not S1PR1, are likely to participate in S1P-induced moesin phosphorylation. In the present study, it was demonstrated that the S1PR2 antagonist, but not S1PR1 or S1PR3 antagonists, abolished the effect of S1P on moesin phosphorylation. These results suggested that high-dose S1P induced moesin phosphorylation via S1PR2 rather than S1PR1 or S1PR3. Furthermore, moesin depletion ameliorated S1P-induced F-actin rearrangement and stress fiber formation, as well as endothelial barrier disruption. Collectively, the data suggested that high-dose S1P induced moesin phosphorylation via S1PR2, and thus mediated endothelial barrier disruption responses. These findings were consistent with a previous report that suggested that S1P-induced cytoskeletal rearrangement was dependent on ERM phosphorylation, with the involvement of S1PR2 (28).

The discrepant effect between low- and high-dose S1P may result from the different roles of S1PRs and ERM proteins. The basic expression level of S1PR2 in endothelial cells was much lower than S1PR1 and S1PR3 (29). A previous study demonstrated that physiological doses of S1P enhanced the TER of the endothelial monolayer, whereas an S1PR1 antagonist significantly attenuated this effect (14). By contrast, high-dose S1P triggered a decrease in the TER value, whereas

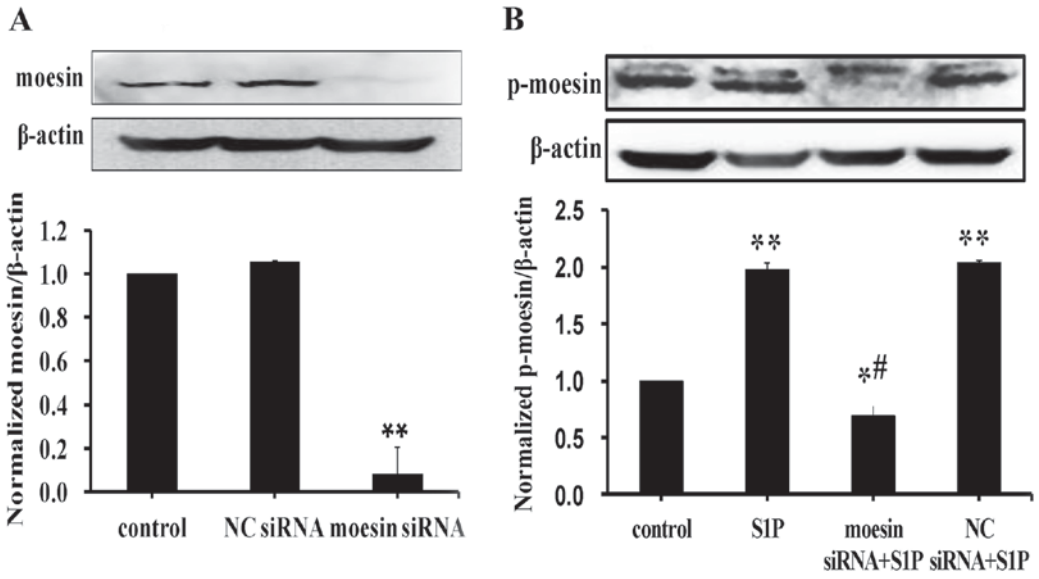

Figure 3. Knockdown of moesin using siRNA abolishes excessive S1P-induced moesin phosphorylation. HUVECs were (A) either untreated (control) or treated with negative control siRNA or siRNA targeting moesin, and (B) subsequently treated with or without S1P. The expression levels of threonine-phosphorylated moesin or β-actin was examined using western blot analysis. The densitometric results are expressed as the mean ± standard deviation from three independent experiments. *P<0.05 vs. untreated control; **P<0.01 vs. untreated control; #P<0.05 vs. NC siRNA+S1P. NC, negative control; siRNA, small interfering RNA; S1P, sphingosine-1-phosphate; p-, phosphorylated.

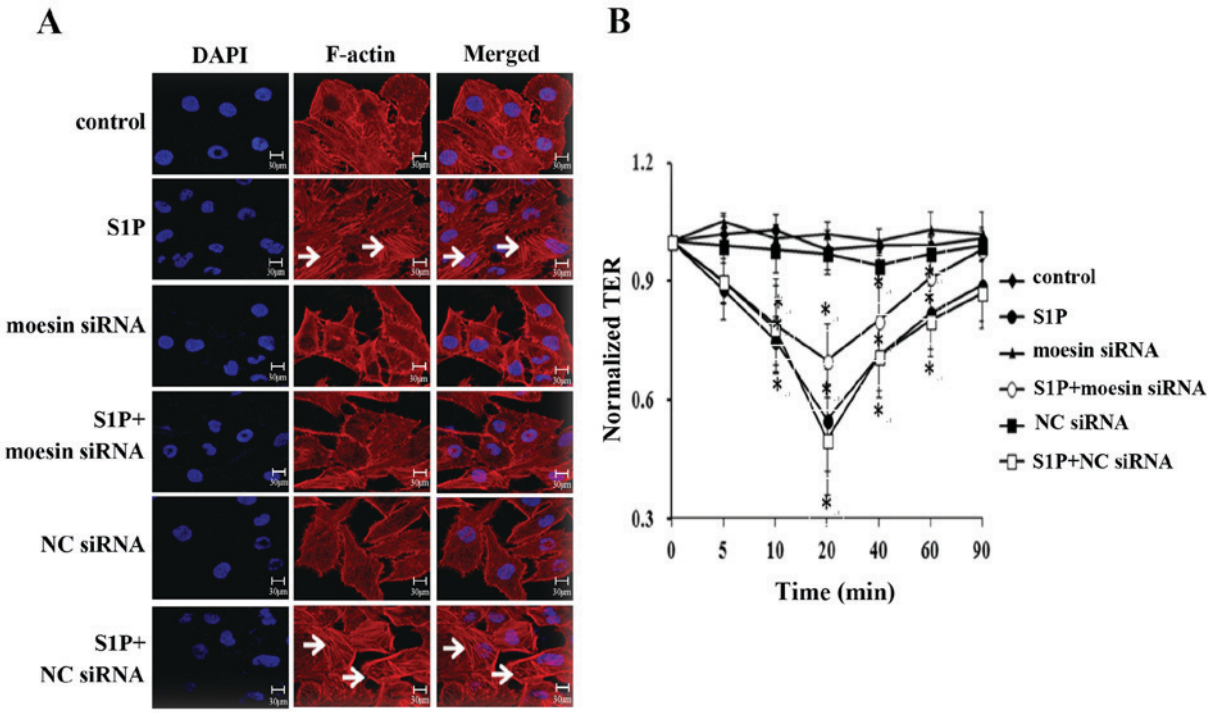

Figure 4. Role of moesin phosphorylation in high-dose S1P-induced endothelial hyperpermeability. HUVECs were untreated (control) or treated with NC siRNA or moesin siRNA, and then stimulated with or without S1P. (A) Cells were fixed and immunofluorescent staining was performed. Cells were probed with rodamine-phalloidin to detect actin filaments (red, marked with white arrows) and with DAPI to label the nucleus (blue). Scale bar, 30 μm. Results are representative of three independent experiments. (B) TER was examined with an EVOM^2 meter and a STX2 electrode. The results are expressed as the mean ± standard deviation from three independent experiments. *P<0.05 vs. untreated control. S1P, sphingosine-1-phosphate; NC, negative control; siRNA, small interfering RNA; TER, transendothelial electrical resistance.

an S1PR2 inhibitor partially ameliorated this effect (14). Therefore, the present study hypothesized that when low-dose S1P encountered those receptors, most of which may bind to S1PR1, prominently mediating a barrier-protective effect. However, when high-dose S1P overwhelmed these receptors, more S1PR2 and S1PR3 were activated and exerted the opposite effect. It was previously unveiled that Rho-associated protein kinase (ROCK) activation served an important role in high-dose S1P-mediated endothelial hyperpermeability through S1PR2 (27). In addition, ROCK activation was

indispensable for AGE-induced moesin phosphorylation (18). Thus, it was speculated that moesin may act as a downstream molecule of the S1PR2-ROCK axis and mediate high-dose S1P-induced endothelial barrier disruption.

How individual ERM proteins differentially regulate endothelial barrier requires further investigation. Adyshev *et al* (27) reported that transfection with either radixin or pan-ERM markedly ameliorated physiological-dose S1P-mediated endothelial barrier enhancement. Ezrin depletion partially attenuated S1P-induced endothelial barrier enhancement and cytoskeletal alterations (27). Moesin was phosphorylated under physiological doses of S1P stimulation; however, the depletion of moesin contributed to the elevated TER value (27). In the present study, it was demonstrated that moesin phosphorylation resulted in high-dose S1P-induced F-actin polymerization, stress fiber formation and endothelial barrier dysfunction, which were dependent on S1PR2.

Taken together, it is possible that under low-dose S1P treatment, radixin serves a key barrier-enhancing role and this process may be associated with S1PR1. Whereas under excessive S1P stimulation, S1PR2 was dominantly activated and mediated moesin-exerted endothelial barrier disruption, and this process may be associated with ROCK activation.

It should be noted that the present study only examined the effect of excessive S1P on endothelial integrity *in vitro*, and it has not yet been investigated *in vivo*. In an LPS-induced murine model of acute lung injury, intravenous injection of S1P (85 μg/kg) significantly rescued vascular leak (30). However, the specific high dose of S1P for *in vivo* study remains to be investigated. As reported previously, the effectiveness of high-dose S1P may be more complex *in vivo*, as S1PR2 expression was upregulated in certain inflammatory conditions (29). The possibility exists that excessive S1P combines with inducible S1PR2 and exacerbates inflammatory responses. The authors of the present study intend to investigate whether excessive S1P functions synergistically with inflammatory mediators such as lipopolysaccharide-binding protein or tumor necrosis factor-α.

In conclusion, the present study suggested that induction of moesin phosphorylation by excessive S1P occurs through S1PR2 and further induces endothelial barrier damage responses. The findings further highlighted the potential utility of a pharmacological target of the S1PR2-moesin axis in vascular barrier dysfunction.

Acknowledgements

The present study was supported by the General Program from Natural Science Foundation of China (grant nos. 81370226 and 81170297) and The Team-Project of Natural Science Foundation of Guangdong, China (grant no. S2013030013217).

References

1. Yoo H, Ku SK, Baek YD and Bae JS: Anti-inflammatory effects of rutin on HMGB1-induced inflammatory responses in vitro and in vivo. Inflamm Res 63: 197-206, 2014.
2. Chen S, Yang J, Xiang H, Chen W, Zhong H, Yang G, Fang T, Deng H, Yuan H, Chen AF and Lu H: Role of sphingosine-1-phosphate receptor 1 and sphingosine-1-phosphate receptor 2 in hyperglycemia-induced endothelial cell dysfunction. Int J Mol Med 35: 1103-1108, 2015.
3. Yatomi Y, Ruan F, Hakomori S and Igarashi Y: Sphingosine-1-phosphate: A platelet-activating sphingolipid released from agonist-stimulated human platelets. Blood 86: 193-202, 1995.
4. Hänel P, Andréani P and Gräler MH: Erythrocytes store and release sphingosine 1-phosphate in blood. FASEB J 21: 1202-1209, 2007.
5. Hisano Y, Kobayashi N, Yamaguchi A and Nishi T: Mouse SPNS2 functions as a sphingosine-1-phosphate transporter in vascular endothelial cells. PloS One 7: e38941, 2012.
6. Nijnik A, Clare S, Hale C, Chen J, Raisen C, Mottram L, Lucas M, Estabel J, Ryder E, Adissu H, *et al*: The role of sphingosine-1-phosphate transporter Spns2 in immune system function. J immunol 189: 102-111, 2012.
7. Liu X, Wu W, Li Q, Huang X, Chen B, Du J, Zhao K and Huang Q: Effect of sphingosine 1-phosphate on morphological and functional responses in endothelia and venules after scalding injury. Burns 35: 1171-1179, 2009.
8. Sanchez T and Hla T: Structural and functional characteristics of S1P receptors. J Cell Biochem 92: 913-922, 2004.
9. Singleton PA, Dudek SM, Chiang ET and Garcia JG: Regulation of sphingosine 1-phosphate-induced endothelial cytoskeletal rearrangement and barrier enhancement by S1P1 receptor, PI3 kinase, Tiam1/Rac1, and alpha-actinin. FASEB J 19: 1646-1656, 2005.
10. Sanchez T: Sphingosine-1-Phosphate signaling in endothelial disorders. Curr Atheroscler Rep 18: 31, 2016.
11. Liu W, Liu B, Liu S, Zhang J and Lin S: Sphingosine-1-phosphate receptor 2 mediates endothelial cells dysfunction by PI3K-Akt pathway under high glucose condition. Eur J Pharmacol 776: 19-25, 2016.
12. Kim GS, Yang L, Zhang G, Zhao H, Selim M, McCullough LD, Kluk MJ and Sanchez T: Critical role of sphingosine-1-phosphate receptor-2 in the disruption of cerebrovascular integrity in experimental stroke. Nat Commun 6: 7893, 2015.
13. Zhang G, Yang L, Kim GS, Ryan K, Lu S, O'Donnell RK, Spokes K, Shapiro N, Aird WC, Kluk MJ, *et al*: Critical role of sphingosine-1-phosphate receptor 2 (S1PR2) in acute vascular inflammation. Blood 122: 443-455, 2013.
14. Li Q, Chen B, Zeng C, Fan A, Yuan Y, Guo X, Huang X and Huang Q: Differential activation of receptors and signal pathways upon stimulation by different doses of sphingosine-1-phosphate in endothelial cells. Exp Physiol 100: 95-107, 2015.
15. Sammani S, Moreno-Vinasco L, Mirzapoiazova T, Singleton PA, Chiang ET, Evenoski CL, Wang T, Mathew B, Husain A, Moitra J, *et al*: Differential effects of sphingosine 1-phosphate receptors on airway and vascular barrier function in the murine lung. Am J Respir Cell Mol Biol 43: 394-402, 2010.
16. Canals D, Jenkins RW, Roddy P, Hernández-Corbacho MJ, Obeid LM and Hannun YA: Differential effects of ceramide and sphingosine 1-phosphate on ERM phosphorylation: Probing sphingolipid signaling at the outer plasma membrane. J Biol Chem 285: 32476-32485, 2010.
17. Adyshev DM, Dudek SM, Moldobaeva N, Kim KM, Ma SF, Kasa A, Garcia JG and Verin AD: Ezrin/radixin/moesin proteins differentially regulate endothelial hyperpermeability after thrombin. Am J Physiol Lung Cell Mol Physiol 305: L240-L255, 2013.
18. Guo X, Wang L, Chen B, Li Q, Wang J, Zhao M, Wu W, Zhu P, Huang X and Huang Q: ERM protein moesin is phosphorylated by advanced glycation end products and modulates endothelial permeability. Am J Physiol Heart Circ Physiol 297: H238-H246, 2009.
19. Patabendige A, Skinner RA and Abbott NJ: Establishment of a simplified in vitro porcine blood-brain barrier model with high transendothelial electrical resistance. Brain Res 1521: 1-15, 2013.
20. Zhang W, Xu Q, Wu J, Zhou X, Weng J, Xu J, Wang W, Huang Q and Guo X: Role of Src in Vascular Hyperpermeability induced by advanced glycation end products. Sci Rep 5: 14090, 2015.
21. Maceyka M, Milstien S and Spiegel S: Sphingosine-1-phosphate: The Swiss army knife of sphingolipid signaling. J Lipid Res 50 (Suppl): S272-S276, 2009.
22. Russo SB, Ross JS and Cowart LA: Sphingolipids in obesity, type 2 diabetes, and metabolic disease. Handb Exp Pharmacol 373-401, 2013.
23. Finigan JH, Dudek SM, Singleton PA, Chiang ET, Jacobson JR, Camp SM, Ye SQ and Garcia JG: Activated protein C mediates novel lung endothelial barrier enhancement: Role of sphingosine 1-phosphate receptor transactivation. J Biol Chem 280: 17286-17293, 2005.
24. Feistritzer C and Riewald M: Endothelial barrier protection by activated protein C through PAR1-dependent sphingosine 1-phosphate receptor-1 crossactivation. Blood 105: 3178-3184, 2005.

25. Garcia JG, Liu F, Verin AD, Birukova A, Dechert MA, Gerthoffer WT, Bamberg JR and English D: Sphingosine 1-phosphate promotes endothelial cell barrier integrity by Edg-dependent cytoskeletal rearrangement. J Clin Invest 108: 689-701, 2001.
26. Schaphorst KL, Chiang E, Jacobs KN, Zaiman A, Natarajan V, Wigley F and Garcia JG: Role of sphingosine-1 phosphate in the enhancement of endothelial barrier integrity by platelet-released products. Am J Physiol Lung Cell Mol Physiol 285: L258-L267, 2003.
27. Adyshev DM, Moldobaeva NK, Elangovan VR, Garcia JG and Dudek SM: Differential involvement of ezrin/radixin/moesin proteins in sphingosine 1-phosphate-induced human pulmonary endothelial cell barrier enhancement. Cell Signal 23: 2086-2096, 2011.
28. Gandy KA, Canals D, Adada M, Wada M, Roddy P, Snider AJ, Hannun YA and Obeid LM: Sphingosine 1-phosphate induces filopodia formation through S1PR2 activation of ERM proteins. Biochem J 449: 661-672, 2013.
29. Du J, Zeng C, Li Q, Chen B, Liu H, Huang X and Huang Q: LPS and TNF-alpha induce expression of sphingosine-1-phosphate receptor-2 in human microvascular endothelial cells. Pathol Res Pract 208: 82-88, 2012.
30. McVerry BJ, Peng X, Hassoun PM, Sammani S, Simon BA and Garcia JG: Sphingosine 1-phosphate reduces vascular leak in murine and canine models of acute lung injury. Am J Respir Crit Care Med 170: 987-993, 2004.